Homotopy Continuation for Feedback Linearization of Noncontact Magnetic Manipulators

Nayereh Riahi, Luis R. Tituaña, and Arash Komaee

Abstract -- Magnetic fields render a unique ability to control magnetic objects without a direct mechanical contact. To exploit this potential for a broad range of medical, microrobotics, and microfluidics applications, noncontact magnetic manipulators have been designed using both electromagnets and permanent magnets. By feedback control of these manipulators, magnetic objects can be precisely driven in the directions required by an application of interest. The feedback design process for these manipulators is normally complicated by their highly nonlinear nature, particulary for those utilizing permanent magnets. Yet, feedback linearization techniques can be applied to compensate for the nonlinear nature of most magnetic manipulators. This goal can be achieved by solving an underdetermined system of nonlinear algebraic equations. This paper adopts a homotopy continuation approach to solve this system of equations. It is shown by simulations that the proposed feedback linearization scheme drastically improves the control performance compared to the alternative control design methods used in prior work.

I. Introduction

This paper concentrates on feedback control of noncontact magnetic manipulators. These apparatus utilize arrangements of multiple magnets to produce and flexibly control magnetic fields, which interact with magnetic objects or fluids in their region of influence in order to control them from a distance without direct mechanical contact. The noncontact feature of magnetic manipulators presents a unique means for operation of magnetically driven tools inside the human body for non-or minimally invasive medical procedures [1]–[12]. Further, noncontact actuation and control are essential components of micro- and nano-scale systems [13]–[18].

By means of feedback control, magnetic manipulators are able to precisely drive magnetic objects in the directions that are required to perform a certain control task such as tracking a reference trajectory at a desired speed [19]–[22]. The major difficulty in design of such feedback control is the nonlinear nature of magnetic manipulators. Yet, the specific structure of nonlinearity in magnetic manipulators allows the use of feedback linearization techniques to effectively compensate for the nonlinearity [19]–[22]. The method used for feedback linearization of magnetic manipulators relies on the solutions to an underdetermined set of nonlinear algebraic equations. This paper proposes a *homotopy continuation* [23] approach for solving this set of algebraic equations.

A homotopy between two vector functions is a parametric family of vector functions with a scalar parameter ranging in

This work was supported by the National Science Foundation under Grant ECCS-1941944.

The authors are with the Department of Electrical and Computer Engineering, Southern Illinois University, Carbondale, IL, 62901 USA email: {nayereh.riahi, luis.tituana, akomaee}@siu.edu.

a closed interval. Varying this parameter from one end of the interval to another end results in continuous deformation of the first vector function toward the second. This continuous deformation creates a continuous trajectory of isolated roots of the family members extended from one end to another. This continuous trajectory satisfies some known differential equation that can be numerically solved with the root of one vector function as its initial condition to determine one root of the other vector function. Therefore, if one vector function is chosen to have a trivial root, an isolated root of the other vector function can be obtained easily.

To demonstrate the feedback linearization method of this paper, a permanent magnet manipulator is utilized, which we recently introduced as an alternative to the more conventional electromagnet manipulators [22]. In our proposed magnetic manipulator, the magnetic field is generated by an array of permanent magnets, and control over magnetic field is gained by mechanical movement of these magnets. The conventional electromagnet manipulators have a rather simpler structure, utilizing a spatially fixed array of electromagnets controlled by their terminal voltages [19]-[21], [24]-[27]. Despite this simple structure, electromagnets of reasonable size and cost may not be capable to produce strong enough magnetic fields for medical applications that typically require large magnetic forces at relatively far distances (several decimeters). On the other hand, permanent magnets offer a much higher strength to size ratio [28], which can be exploited to develop more compact, less expensive magnetic manipulators.

In Section II, the magnetic manipulator in [22] is briefly described and a nonlinear state-space equation governing its dynamics is presented. In Section III, the proposed feedback linearization technique is applied to this state-space equation to transform it into an equivalent linear system, for which a linear controller is designed by the method of linear quadratic regulator. Combining this linear controller with the nonlinear transformation introduced by feedback linearization results in an overall nonlinear controller, which enables the magnetic manipulator to precisely drive a magnetic particle along any arbitrary reference trajectory. Computation of this nonlinear transformation using homotopy continuation is considered in Section IV. The performance of proposed control is evaluated in Section V using computer simulations, which demonstrate that feedback linearization significantly improves the control performance compared to a simple control developed in [22].

II. MODEL AND PROBLEM STATEMENT

In a recent paper, we presented the conceptual design of a class of permanent magnet manipulators [22]. Currently, we



Fig. 1: Experimental magnetic manipulator with 6 diametrically magnetized permanent magnet discs. The permanent magnets can freely rotate a full 360 degrees inside their guiding cylinders using 6 independent servomotors. By properly adjusting the directions of all magnets, the magnetic field inside a circular container can be flexibly shaped to precisely steer a magnetic bead along arbitrary reference trajectories.

are developing an experimental setup to evaluate this class of magnetic manipulators in practice (in the near future). Fig. 1 shows the first prototype of this experimental setup.

The setup in this figure consists of a circular flat container and an arrangement of diametrically magnetized permanent magnet discs placed around the container at equal distances. The container is filled with a thin layer of viscous fluid, and a magnetic bead moves inside the fluid. The fluid layer is thin enough to confine the magnetic bead in a plane. Each magnet is rotated by an individual servomotor to control its direction independently. The servomotors are equipped with internal feedback control that enables them to rapidly and precisely adjust the direction of magnets as requested. By appropriate adjustment of the directions of all magnets, the total magnetic field, and as a result, the total magnetic force applied to the magnetic bead can be arbitrarily controlled. Then, by means of feedback control, the magnetic bead can be driven along arbitrary reference trajectories. To establish feedback control, the instantaneous position and velocity of the magnetic bead are measured by a real-time sensing device (not shown in Fig. 1), such as a high-speed camera equipped with image processing and tracking algorithms.

We developed a nonlinear state-space equation in [22] to describe the dynamics of magnetic bead in the manipulator of Fig. 1. To keep the paper self-contained, this state-space equation is reproduced here without details of derivation. The state vector in this equation contains the position $r(t) \in \mathbb{R}^2$ and the velocity $v(t) \in \mathbb{R}^2$ of the magnetic bead in its plane of motion. These vectors are presented in a planar orthogonal coordinate system with the origin at the center of the circular container and a fixed orientation with respect to the magnetic manipulator, as shown in Fig. 2(a). The control $\theta(t) \in \mathbb{R}^n$ is a vector containing the directions of n magnets employed by the magnetic manipulator (n = 6 in Fig. 1). The direction of magnet $k = 1, 2, \dots, n$ is described by an angle θ_k measured counterclockwise between its north pole and a fixed vector ρ_k extended from the center of coordinate system toward the center of magnet, as shown in Fig. 2(b). The control vector is then given by $\theta = (\theta_1, \theta_2, \dots, \theta_n)$.

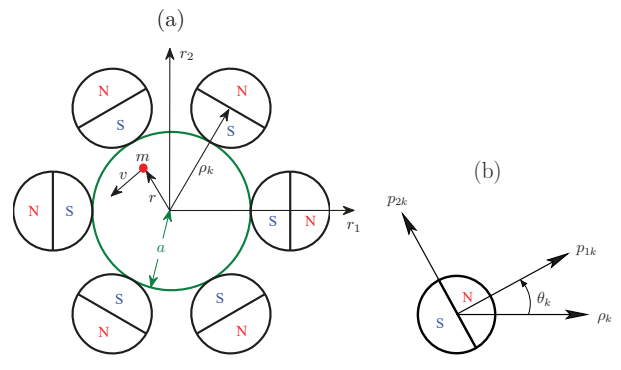


Fig. 2: Magnetic manipulator with n=6 diametrically magnetized discs of radius b equally spaced around a circular flat container of radius a: (a) reference coordinate system r_1-r_2 ; (b) local coordinate system $p_{1k}-p_{2k}$ for magnet k with a rotation angle θ_k .

The dynamics of magnetic bead in the experimental setup of Fig. 1 is governed by Newton's second law of motion, and incorporates the contribution of both magnetic force and fluid resistance (drag). This dynamics is represented by the set of state-space equations

$$\dot{r}\left(t\right) = v\left(t\right) \tag{1a}$$

$$\dot{v}(t) = -\sigma v(t) + \alpha g(r(t), \theta(t)), \qquad (1b)$$

where $g\left(\cdot\right):\mathbb{R}^{2}\times\mathbb{R}^{n}\to\mathbb{R}^{2}$ is a vector function and σ and α are positive constants. The linear term $-\sigma v\left(t\right)$ on the right-hand side of (1b) represents the drag force normalized to the mass of the magnetic bead, while the nonlinear term $\alpha g\left(\cdot\right)$ is the normalized magnetic force. For detailed description of the parameters σ and α , the interested reader is referred to [22].

Suppose that $h\left(r,\theta\right)$ is the total magnetic field generated by n magnets at a point r under a control vector θ . The vector function $g\left(\cdot\right)$ in the state-space equation (1b) is defined as

$$g(r, \theta) = \nabla \|h(r, \theta)\|^2$$

where ∇ is the operator of gradient with respect to r and $\|\cdot\|$ stands for the Euclidean norm of vectors. The total magnetic field is the superposition of magnetic fields generated by n magnets, and is explicitly given in [22] by

$$h(r,\theta) = \sum_{k=1}^{n} R_k^T(\theta_k) h_c(R_k(\theta_k)(r - \rho_k)).$$
 (2)

Here, $R_k(\cdot)$, k = 1, 2, ..., n is the rotation matrix

$$R_k(\phi) = \begin{bmatrix} \cos\left(\phi + \frac{2\pi(k-1)}{n}\right) & \sin\left(\phi + \frac{2\pi(k-1)}{n}\right) \\ -\sin\left(\phi + \frac{2\pi(k-1)}{n}\right) & \cos\left(\phi + \frac{2\pi(k-1)}{n}\right) \end{bmatrix}$$

and ρ_k , k = 1, 2, ..., n is the 2×1 vector

$$\rho_k = (a+b) \left[\cos \frac{2\pi(k-1)}{n} \quad \sin \frac{2\pi(k-1)}{n} \right]^T,$$

where a and b are the radii of the circular container and the permanent magnet discs, respectively.

In the total magnetic field (2), $h_c(\cdot): \mathbb{R}^2 \to \mathbb{R}^2$ represents the magnetic field of each permanent magnet disc in its own coordinate system. As shown in Fig. 2(b), a local coordinate system is fixed to each magnet with the origin at the center of magnet and the first orthogonal axis aligned with its north

pole. For any point p in that local coordinate system, $h_c\left(p\right)$ represents the magnetic field generated at p by that individual magnet. An analytic form of $h_c\left(\cdot\right)$ has been proposed in [29], which is adopted in this paper for both controller design and numerical simulations. In a recent study, we experimentally verified this analytic form by showing that its values closely match the empirical data collected by a magnetic mapper.

A. Statement of Control Problem

The purpose of this paper is to develop a feedback control law that enables the magnetic manipulator of Fig. 1 to steer a magnetic object along a desired reference trajectory inside its region of influence (circular container) $\mathscr{C} \subset \mathbb{R}^2$. The specific goal is to develop a state feedback of the form

$$\theta(t) = \mu(r(t), v(t), r_d(t)) \tag{3}$$

to control the state-space equations (1) in such a manner that the position vector $r\left(t\right)$ closely tracks a continuous reference trajectory $r_d\left(t\right)$. Here, $\mu\left(\cdot\right):\mathbb{R}^2{\times}\mathbb{R}^2{\times}\mathbb{R}^2\to\mathbb{R}^n$ is a control law which in general is a nonlinear function, and $r_d\left(t\right)\in\mathscr{C}$ is any continuous function of time that represents a trajectory inside the region of influence of the magnetic manipulator.

To improve the performance of feedback, the memoryless control law (3) can be upgraded to a dynamical system that includes integral, derivative, or lead-lag actions. Even though this paper focuses on the state feedback (3) for the purpose of computer simulations, the feedback linearization technique proposed in Section III can be identically applied for design of such dynamic feedback laws.

III. CONTROL DESIGN BY FEEDBACK LINEARIZATION

In design of feedback law for the state-space equations (1), a major challenge is the nonlinear structure of these equations caused by the nonlinear function $g\left(\cdot\right)$. On the other hand, the large number of control variables in a magnetic manipulator makes it possible to compensate for its nonlinearity, at least within some region of operation. For a magnetic manipulator with at least n=3 magnets, $g\left(r,\theta\right)$ is a 2-dimensional vector while θ is at least 3-dimensional. Thus, the algebraic equation

$$g\left(r,\theta\right) = z\tag{4}$$

is underdetermined and admits infinitely many solutions for θ if the constant parameters $r \in \mathbb{R}^2$ and $z \in \mathbb{R}^2$ are taken from a certain subset of $\mathbb{R}^2 \times \mathbb{R}^2$. In the remainder of this paper, \mathscr{S} denotes the largest subset of $\mathbb{R}^2 \times \mathbb{R}^2$ such that the algebraic equation (4) admits at least one solution for each $(r, z) \in \mathscr{S}$.

For any value of the pair (r,z) taken from \mathscr{S} , the algebraic equation (4) has a solution for θ that depends on (r,z), and can be expressed as $\theta=g^{-1}\left(r,z\right)$. Here, $g^{-1}\left(\cdot\right):\mathscr{S}\to\mathbb{R}^n$ is a nonlinear vector function regarded as the inverse of $g\left(\cdot\right)$ in the sense that

$$g\left(r,g^{-1}\left(r,z\right)\right)=z,\quad (r,z)\in\mathscr{S}.$$
 (5)

Obviously, the inverse function is nonunique and in general, infinitely many of them exist.

Feedback linearization of magnetic manipulators relies on the inverse function $g^{-1}\left(\cdot\right)$ based on the concept illustrated

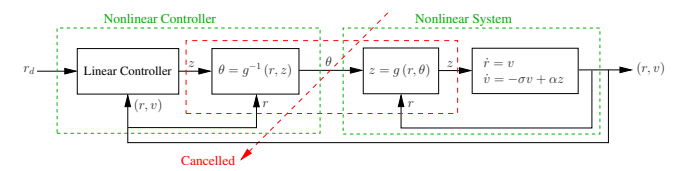


Fig. 3: An essentially nonlinear magnetic manipulator is controlled under a nonlinear feedback in such a manner that the nolinearity of the feedback controller compensates for the nonlinearity of the magnetic manipulator, so that the overall closed-loop system virtually behaves as a linear system.

in the block diagrams of Fig. 3. Consider an auxiliary control vector $z\left(t\right)\in\mathbb{R}^{2}$ and apply a control of the form

$$\theta(t) = g^{-1}(r(t), z(t)) \tag{6}$$

to the state-space equations (1). By definition (5) for $g^{-1}(\cdot)$, this feedback control transforms the nonlinear system (1) into the linear system

$$\dot{r}(t) = v(t)$$

$$\dot{v}(t) = -\sigma v(t) + \alpha z(t)$$
(7)

with a new control z(t). Of course, this linear model is only applicable to those state and control trajectories that satisfy

$$(r(t), z(t)) \in \mathscr{S}$$
 (8)

during the entire course of control.

As shown in Fig. 3, the purposeful nonlinearity introduced via transformation (6) entirely compensates for the intrinsic nonlinearity of the magnetic manipulator such that the overall closed-loop system behaves as a linear system. Therefore, the control design problem for an essentially nonlinear magnetic manipulator is reduced to design of a linear controller for the linear system described by the state-space equations (7). This controller must be designed in such a manner that in normal mode of operation, it only yields state and control trajectories that satisfy (8). The linear controller can be designed either as a memoryless state feedback, or for higher performance, as a dynamical system involving integral, derivative, or any other filtering actions. After developing a suitable linear controller using any standard design method, this controller is cascaded with the nonlinear memoryless system (6) in order to develop a nonlinear control law applied to the magnetic manipulator.

To develop a state feedback law of the form (3), the linear controller adopted in this paper is the linear state feedback

$$z(t) = -K_r(r(t) - r_d(t)) - K_v v(t), \qquad (9)$$

where K_r and K_v are 2×2 gain matrices. The optimal values of these gain matrices are determined using a linear quadratic regulator approach (see [22] for the details). Combining this linear controller with the nonlinear transformation (6) leads to the nonlinear state feedback law

$$\mu(r, v, r_d) = g^{-1}(r, -K_r(r - r_d) - K_v v). \tag{10}$$

This control law is defined only for those vales of (r, v, r_d) for which the inverse function $g^{-1}(\cdot)$ exists. For this reason, the linear mode of closed-loop operation is restricted only to a subregion rather than the entire region of influence of the magnetic manipulator, as discussed in Section V.

Practical implementation of the nonlinear control law (10) relies on the numerical values of the inverse function $g^{-1}(\cdot)$, which must be computed in real time by solving the algebraic equation (4) for θ . This underdetermined equation typically admits infinitely many solutions that can be equally taken as a value of the inverse function. In practice, however, certain solutions may be preferred to others for technical reasons. In our prior work [22], we proposed to select the most preferred solution by solving certain constrained optimization problem.

An alternative approach adopted in this paper attempts to compute a solution of (4) with minimal computational effort, which is suitable for real-time implementation. Furthermore, this solution is constructed in such a manner that effectively reduces the rate of change of θ (t). It is reminded that θ (t) is the input signal applied to servomotors, which are low-pass systems in nature with practical limitations on their slew rate. Thus, a slower reference signal θ (t) elevates the performance of servomotors, and as a consequence, the overall closed-loop performance of the magnetic manipulator.

IV. HOMOTOPY CONTINUATION

This paper adopts the concept of homotopy continuation to solve the nonlinear algebraic equation (4). The advantage of this approach over its alternatives such as Newton's method is that its convergence to a solution of (4) barely depends on the choice of initial guess for the solution [30]. This property is in particular important for the real-time application of this paper, which requires to frequently solve a complex equation under different parameter values without reliance on human intelligence to identify a suitable initial guess. In the rest of this section, the concept of homotopy continuation is briefly discussed and it is applied to the algebraic equation (4).

Suppose $f(\cdot): \mathbb{R}^n \to \mathbb{R}^m$, $m \le n$ is a vector function and the goal is to solve the algebraic equation f(w) = 0. When a simple solution to this problem is not known, an alternative is to use the method of homotopy described below. Consider another vector function $f_0(\cdot): \mathbb{R}^n \to \mathbb{R}^m$ that has a known solution w_0 satisfying $f_0(w_0) = 0$. Take a scalar parameter s and construct the family of vector functions

$$F(w,s) = sf(w) + (1-s) f_0(w), \quad s \in [0,1],$$

which is called a homotopy between $f(\cdot)$ and $f_0(\cdot)$. For the purpose of solving f(w) = 0, any other family of functions that holds two conditions $f(\cdot) = F(\cdot, 1)$ and $F(w_0, 0) = 0$ can be equivalently employed.

Suppose w(s), $s \in [0,1]$ is a continuous trajectory of the solutions to the family of algebraic equations

$$F(w(s), s) = 0, \quad s \in [0, 1].$$

This trajectory has the key properties that its value at s=1 solves the algebraic equation $f\left(w\right)=0$, and additionally, the entire trajectory $w\left(s\right),\ s\in\left[0,1\right]$ is the solution to the initial value problem

$$\frac{d}{ds} F(w(s), s) = 0, \quad s \in [0, 1]$$
(11a)

$$w(0) = w_0,$$
 (11b)

provided that $F\left(\cdot\right)$ is differentiable. Hence, this problem can be solved on $s\in\left[0,1\right]$ to obtain $w\left(1\right)$ that solves $f\left(w\right)=0$. The explicit form of (11a) is given by

$$F_w(w(s), s) w'(s) + F_s(w(s), s) = 0,$$
 (12)

where $w'\left(\cdot\right)$ is the derivative of $w\left(\cdot\right)$, and $F_{w}\left(\cdot\right)$ and $F_{s}\left(\cdot\right)$ denote the Jacobian matrices of $F\left(w,s\right)$ with respect to w and s, respectively. This equation is linear in $w'\left(s\right)$, which is explicitly solved to obtain the standard form

$$w'(s) = -F_w^{\dagger}(w(s), s) F_s(w(s), s),$$
 (13)

where $F_w^{\dagger}(\cdot)$ denotes the inverse of $F_w(\cdot)$ when m=n, and its Moore-Penrose inverse for m< n. The solution to (12) is not unique when m< n, and (13) is only a possible solution. Yet, this particular solution is computationally least complex, as any other solution introduces an extra additive term on the right-hand side of (13).

For solving the algebraic equation (4), fix the parameters r and z, take any arbitrary initial guess $\theta_0 \in \mathbb{R}^n$, and construct the homotopy

$$F(w,s) = g(r,w) - sz - (1-s)g(r,\theta_0).$$

Using this homotopy, a solution of (4) can be determined by solving the initial value problem

$$w'(s) = G_{\theta}^{\dagger}(r, w(s)) \left(z - g(r, \theta_0)\right) \tag{14a}$$

$$w\left(0\right) = \theta_0 \tag{14b}$$

over $s \in [0, 1]$ and taking w(1) as that solution. Here, $G_{\theta}(\cdot)$ is the Jacobian matrix of $g(r, \theta)$ with respect to θ .

The algebraic equation (4) does not admit any solution for certain parameter values $(r,z) \notin \mathscr{S}$. This case is manifested by the abnormal condition that the differential equation (14) becomes singular at some $s=\bar{s}$ in the interval [0,1), i.e., the Moore-Penrose inverse $G_{\theta}^{\dagger}(r,w(\bar{s}))$ becomes nonexistent. In this case, $w(\bar{s})$ is taken as a reasonable replacement for the nonexistent value of the inverse function $g^{-1}(r,z)$.

The initial guess θ_0 in the differential equation (14) can be taken arbitrarily; however, by choosing its value smartly, two key advantages are achieved simultaneously. Suppose that the control θ (t) is updated at a sampling rate T, i.e., the values of θ (kT), $k=0,1,2,\ldots$ are generated by solving (4) with the parameters r (kT) and z (kT). Then, to compute θ (kT), the initial guess is taken as $\theta_0 = \theta$ (kT - T). Noting that the parameters r (kT) and z (kT) change slowly with k, for this initial guess, θ (kT) typically stays close to θ (kT - T). This property offers two advantages: effectively reduces the rate of change of θ (t), and lowers the computational cost of solving the initial value problem (14).

V. SIMULATION RESULTS

The closed-loop performance of the magnetic manipulator of Fig. 1 was evaluated by computer simulations developed in Matlab. These simulations numerically solve the state-space equations (1) under a control generated by the state feedback law (10). In parallel, simulation results were produced under an approximate control law, as a baseline for comparison. We

originally proposed this approximate control law in [22] as an inexpensive alternative to the exact control law (10). This control law approximates $q^{-1}(\cdot)$ in (10) with

$$g^{-1}(r,z) \simeq G_{\theta}^{\dagger}(r,0) (z - g(r,0)),$$
 (15)

which is obtained by solving the approximate linear equation

$$g(r,\theta) \simeq g(r,0) + G_{\theta}(r,0)\theta = z.$$

The simulations were designed to study two major issues: closed-loop stability, and tracking performance. The stability issue is in particular important, as the dynamics of magnetic objects inside magnetic fields is intrinsically unstable, which can be stabilized only by means of feedback. Such open-loop instability is an essential property of magnetic manipulators regardless of their type, design, and geometry, a fact directly implied by Earnshaw's theorem [8], [12].

The simulations investigate the asymptotic stability of the equilibrium (r,v)=(0,0) under the control law (10) and its approximation (15). Note that (r,v)=(0,0) is indeed an equilibrium point of (1) under $\theta(t)=0$, since g(0,0)=0 holds by geometric symmetry. In addition, this equilibrium is open-loop unstable, which can be shown by linearizing the state-space equations (1) at the origin and verifying that the linearized system has strictly positive poles.

A. Numerical Results

The simulations were run for a magnetic manipulator with n=6 identical magnets of radius b=0.5 spaced at equal distances around a circle with a normalized radius a=1. The numerical values of parameters in (1) were chosen as $\sigma=1$ and $\alpha=1$. The 2×2 gain matrices K_r and K_v in the linear controller (9) were determined as

$$K_r = \text{diag}(31.6, 31.6), \quad K_v = \text{diag}(7.01, 7.01)$$

by the linear quadratic regulator method (see [22] for details). The magnetic field $h_c\left(\cdot\right)$ of the individual magnets involved in (2) was computed from an analytical formula in [29] for magnets of radius b=0.5 and thickness d=0.1. The rest of parameters in this formula were normalized to result in a unit magnetic field at a unit distance from the magnet poles.

The simulation results demonstrate successful stabilization of the unstable equilibrium at the origin (r,v)=(0,0) under both control laws (10) and its approximate form (15), even though the exact control (10) has a substantially larger region of attraction (ROA). This improvement in the ROA is clearly observed in Fig. 4, which illustrates the cross section of ROA with the hyperplane v=0 for both exact and approximate control laws. This cross section represents a subregion within the region of influence of the magnetic manipulator (circular container) with the following property: under the feedback control (10) with $r_d(t)=0$, any magnetic particle initially stationary inside this subregion moves toward and eventually stops at the center r=0 of the subregion. A typical trajectory of such magnetic particle is illustrated in Fig. 5.

For the magnetic manipulator of Fig. 1, the performance of trajectory tracking under feedback control is studied in Fig. 6. The control goal in this figure is to drive a magnetic bead at a

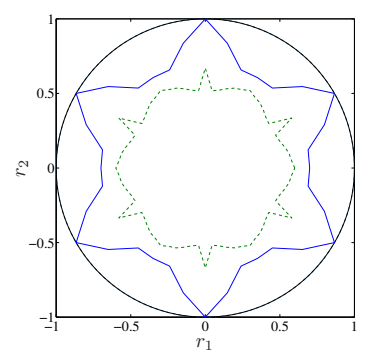


Fig. 4: Cross section of ROA with the hyperplane v=0 for the unstable equilibrium at (r,v)=(0,0) under the exact state feedback (10) (inside solid line) and its approximation (15) (inside dashed line). The approximate control law stabilizes the equilibrium with a smaller ROA. The interior of circle represents the region of influence of the magnetic manipulator.

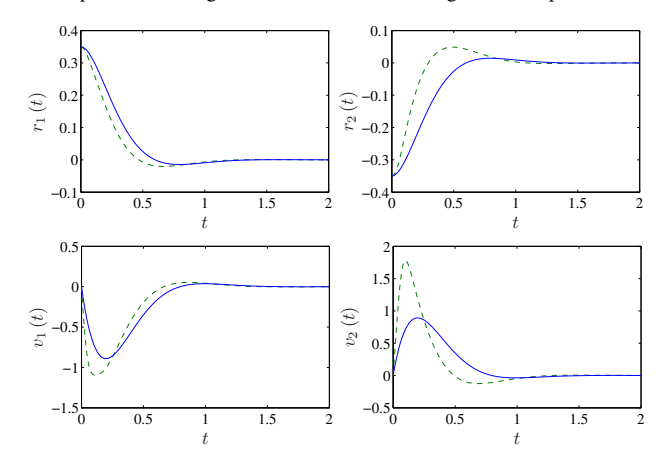


Fig. 5: State trajectories approaching the equilibrium (0,0) under the exact state feedback (10) (solid line) and its approximation (15) (dashed line).

constant speed along a reference trajectory resembling SIU. Fig. 6(a) depicts the trajectory of magnetic bead (solid line) as it tracks the reference trajectory (dash-dotted line) under the feedback law (10). According to Fig. 6(a), this feedback law enables the magnetic manipulator to precisely drive the magnetic bead along a complex trajectory that covers a large area in the region of influence of the magnetic manipulator.

Fig. 6(b) compares the tracking performance of the exact control (10) with its approximation (15) from two points of view. First, this figure indicates that the exact feedback law is able to successfully steer the magnetic bead along reference trajectories covering a much larger area, as compared to its approximate counterpart. Second, the exact feedback law is significantly more precise in tracking reference trajectories. This second property can be also observed in Fig. 7 which illustrates the trajectories of Fig. 6(b) versus time.

VI. CONCLUSION

A feedback linearization technique was introduced in this paper to properly compensate for highly nonlinear dynamics of noncontact magnetic manipulators. This technique mainly relies on the solutions to an underdetermined set of nonlinear algebraic equations. A homotopy continuation approach was adopted to numerically solve this set of nonlinear equations in real time. It was shown via computer simulations that the control law designed by feedback linearization significantly

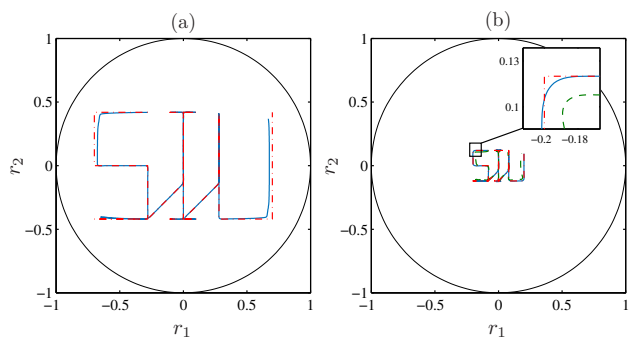


Fig. 6: Magnetic bead tracks a SIU-shaped reference trajectory (dash-dotted line) at a constant speed under (a) the exact control law (10) (solid line), and (b) its approximation (15) (dashed line). The reference trajectory in (b) is the largest possible that the magnetic bead can successfully track under the approximate control law.

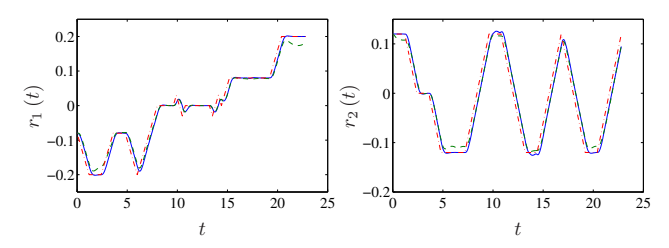


Fig. 7: Trajectory of magnetic bead versus time as it tracks a SIU-shaped reference trajectory (dash-dotted line) under the exact feedback control (10) (solid line) and its approximation (15) (dashed line).

outperforms those designed in the past based on approximate linearization methods.

ACKNOWLEDGMENT

The authors would like to thank Octavio D. Rodriguez for photographing the experimental setup in Fig. 1.

REFERENCES

- M. Sendoh, K. Ishiyama, and K.-I. Arai, "Fabrication of magnetic actuator for use in a capsule endoscope," *IEEE Trans. Magn.*, vol. 39, no. 5, pp. 3232–3234, 2003.
- [2] G. Ciuti, P. Valdastri, A. Menciassi, and P. Dario, "Robotic magnetic steering and locomotion of capsule endoscope for diagnostic and surgical endoluminal procedures," *Robotica*, vol. 28, no. 2, pp. 199– 207, 2010.
- [3] M. Simi, P. Valdastri, C. Quaglia, A. Menciassi, and P. Dario, "Design, fabrication, and testing of a capsule with hybrid locomotion for gastrointestinal tract exploration," *IEEE/ASME Trans. Mechatronics*, vol. 15, no. 2, pp. 170–180, 2010.
- [4] A. Komaee and B. Shapiro, "Magnetic steering of a distributed ferrofluid spot towards a deep target with minimal spreading," in *Proc.* of 50th IEEE Conference on Decision and Control and European Control Conference, pp. 7950–7955, Dec. 2011.
- [5] S. Yim and M. Sitti, "Design and rolling locomotion of a magnetically actuated soft capsule endoscope," *IEEE Trans. Robot.*, vol. 28, no. 1, pp. 183–194, 2012.
- [6] S. Yim and M. Sitti, "Shape-programmable soft capsule robots for semi-implantable drug delivery," *IEEE Trans. Robot.*, vol. 28, no. 5, pp. 1198–1202, 2012.
- [7] G.-S. Lien, C.-W. Liu, J.-A. Jiang, C.-L. Chuang, and M.-T. Teng, "Magnetic control system targeted for capsule endoscopic operations in the stomach—design, fabrication, and in vitro and ex vivo evaluations," *IEEE Trans. Biomed. Eng.*, vol. 59, no. 7, pp. 2068–2079, 2012
- [8] A. Nacev, A. Komaee, A. Sarwar, R. Probst, S. H. Kim, M. Emmert-Buck, and B. Shapiro, "Towards control of magnetic fluids in patients: directing therapeutic nanoparticles to disease locations," *IEEE Control Syst. Mag.*, vol. 32, no. 3, pp. 32–74, 2012.

- [9] A. Komaee, R. Lee, A. Nacev, R. Probst, A. Sarwar, D. A. Depireux, K. J. Dormer, I. Rutel, and B. Shapiro, *Magnetic Nanoparticles: From Fabrication to Clinical Applications*, ch. Putting Therapeutic Nanoparticles Where They Need to Go by Magnet Systems Design and Control, pp. 419–448. CRC Press, 2012.
- [10] M. Beccani, C. Di Natali, L. J. Sliker, J. A. Schoen, M. E. Rentschler, and P. Valdastri, "Wireless tissue palpation for intraoperative detection of lumps in the soft tissue," *IEEE Trans. Biomed. Eng.*, vol. 61, no. 2, pp. 353–361, 2014.
- [11] V. Iacovacci, L. Ricotti, P. Dario, and A. Menciassi, "Design and development of a mechatronic system for noninvasive refilling of implantable artificial pancreas," *IEEE/ASME Trans. Mechatronics*, vol. 20, no. 3, pp. 1160–1169, 2015.
- [12] A. Komaee, "Feedback control for transportation of magnetic fluids with minimal dispersion: A first step toward targeted magnetic drug delivery," *IEEE Trans. Control Syst. Technol.*, vol. 25, no. 1, pp. 129– 144, 2017.
- [13] C. Gosse and V. Croquette, "Magnetic tweezers: Micromanipulation and force measurement at the molecular level," *Biophysical Journal*, vol. 82, no. 6, pp. 3314–3329, 2002.
- [14] M. B. Khamesee, N. Kato, Y. Nomura, and T. Nakamura, "Design and control of a microrobotic system using magnetic levitation," *IEEE/ASME Trans. Mechatronics*, vol. 7, no. 1, pp. 1–14, 2002.
- [15] N. Pamme, "Magnetism and microfluidics," Lab on a Chip, vol. 6, no. 1, pp. 24–38, 2006.
- [16] M. A. M. Gijs, F. Lacharme, and U. Lehmann, "Microfluidic applications of magnetic particles for biological analysis and catalysis," *Chemical Reviews*, vol. 110, no. 3, pp. 1518–1563, 2009.
- [17] S. Schuerle, S. Erni, M. Flink, B. E. Kratochvil, and B. J. Nelson, "Three-dimensional magnetic manipulation of micro- and nanostructures for applications in life sciences," *IEEE Trans. Magn.*, vol. 49, no. 1, pp. 321–330, 2013.
- [18] H. Marino, C. Bergeles, and B. J. Nelson, "Robust electromagnetic control of microrobots under force and localization uncertainties," *IEEE Trans. Autom. Sci. Eng.*, vol. 11, no. 1, pp. 310–316, 2014.
- [19] A. Komaee and B. Shapiro, "Steering a ferromagnetic particle by magnetic feedback control: Algorithm design and validation," in *Proc.* of 2010 American Control Conference (ACC 2010), pp. 6543–6548, 2010.
- [20] R. Probst, J. Lin, A. Komaee, A. Nacev, Z. Cummins, and B. Shapiro, "Planar steering of a single ferrofluid drop by optimal minimum power dynamic feedback control of four electromagnets at a distance," J MAGN MAGN MATER, vol. 323, no. 7, pp. 885–896, 2011.
- [21] A. Komaee and B. Shapiro, "Steering a ferromagnetic particle by optimal magnetic feedback control," *IEEE Trans. Control Syst. Technol.*, vol. 20, no. 4, pp. 1011–1024, 2012.
- [22] N. Riahi and A. Komaee, "Steering magnetic particles by feedback control of permanent magnet manipulators," in *Proc. of 2019 American Control Conference (ACC 2019)*, pp. 5432–5437, 2019.
- [23] E. L. Allgower and K. Georg, Introduction to Numerical Continuation Methods. Philadelphia, PA: Society for Industrial and Applied Mathematics, 2003.
- [24] F. M. Creighton, Control of magnetomotive actuators for an implanted object in brain and phantom materials. PhD thesis, University of Virginia, 1991.
- [25] E. G. Quate, K. G. Wika, M. A. Lawson, G. T. Gillies, R. C. Ritter, M. S. Grady, and M. A. Howard, "Goniometric motion controller for the superconducting coil in a magnetic Stereotaxis system," *IEEE Trans. Biomed. Eng.*, vol. 38, no. 9, pp. 899–905, 1991.
- [26] M. P. Kummer, J. J. Abbott, B. E. Kratochvil, R. Borer, A. Sengul, and B. J. Nelson, "OctoMag: An electromagnetic system for 5-DOF wireless micromanipulation," *IEEE Trans. Robot.*, vol. 26, no. 6, pp. 1006–1017, 2010.
- [27] S. Afshar, M. B. Khamesee, and A. Khajepour, "Optimal configuration for electromagnets and coils in magnetic actuators," *IEEE Trans. Magn.*, vol. 49, no. 4, pp. 1372–1381, 2013.
- [28] O. Baun and P. Blümler, "Permanent magnet system to guide superparamagnetic particles," *J MAGN MAGN MATER*, vol. 439, pp. 294– 304, 2017.
- [29] M. Fontana, F. Salsedo, and M. Bergamasco, "Novel magnetic sensing approach with improved linearity," *Sensors*, vol. 13, no. 6, pp. 7618– 7632, 2013.
- [30] C.-S. Liu, W. Yeih, C.-L. Kuo, and S. N. Atluri, "A scalar homotopy method for solving an over/under-determined system of non-linear algebraic equations," *CMES*, vol. 53, no. 1, p. 47, 2009.